

Earthquake Induced Damage Mitigation from Soil Liquefaction

**CLASS A PREDICTION FOR LIQUEFACTION REMEDIATION
INITIATIVE CENTRIFUGE TEST 6 (LRICT6)**

**By:
Ahmad Jafari**

Supervisor: Dr. Radu Popescu

**Memorial University of Newfoundland
January 2005**

Introduction

In this report Class A prediction of the 6th LRI (Liquefaction Remediation Initiative) centrifuge test (LRICT6) is presented and discussed. The test material consists of uniform loose Fraser River sand. The input motion is A2475 with a magnification factor of 2, i.e. $2 \times A2475$, which has already been reported in the previous class A predictions. General layout of this centrifuge test is shown in Figure 1.

The FE model used in the class A prediction of this test is similar to that of LRICT5 prediction, which consists of 588 nodes and 542 elements. The time step used in the step-by-step dynamic analysis was $\Delta t = 0.02 \text{ sec}$, corresponding to the time step used for the target acceleration time history. The run time for this model on a P4, 2.6GHz PC was about 5 minutes.

The soil properties for loose sand are the same as those used in class A prediction of LRICT5 and for the saturation layer the material properties are similar to the material properties of drainage dykes, provided in class A predictions of LRICT4 and LRICT5.

Results of Class A prediction of LRICT6

Results of class A prediction of the 6th centrifuge test are discussed hereafter. The predicted maximum shear strain contours are shown in Figure 2 along with the deformed shape of the model. Figure 3 shows vertical displacement contours at the end of analysis ($t = 42.56 \text{ s}$). The predicted settlement at upslope free field is larger than 0.4m. Figures 4 to 26 show the predicted responses at different transducers. It is mentioned that the numerical model predicts significant dilation (i.e. large negative excess pore water pressures) between $t = 12 \text{ s}$ and $t = 17 \text{ s}$, especially at very shallow locations (EPP4, EPP5, EPP8 and EPP9). The excessive negative pore pressures predicted at location EPP4 (Figure 11) are believed to be due to the proximity of the lateral boundary.

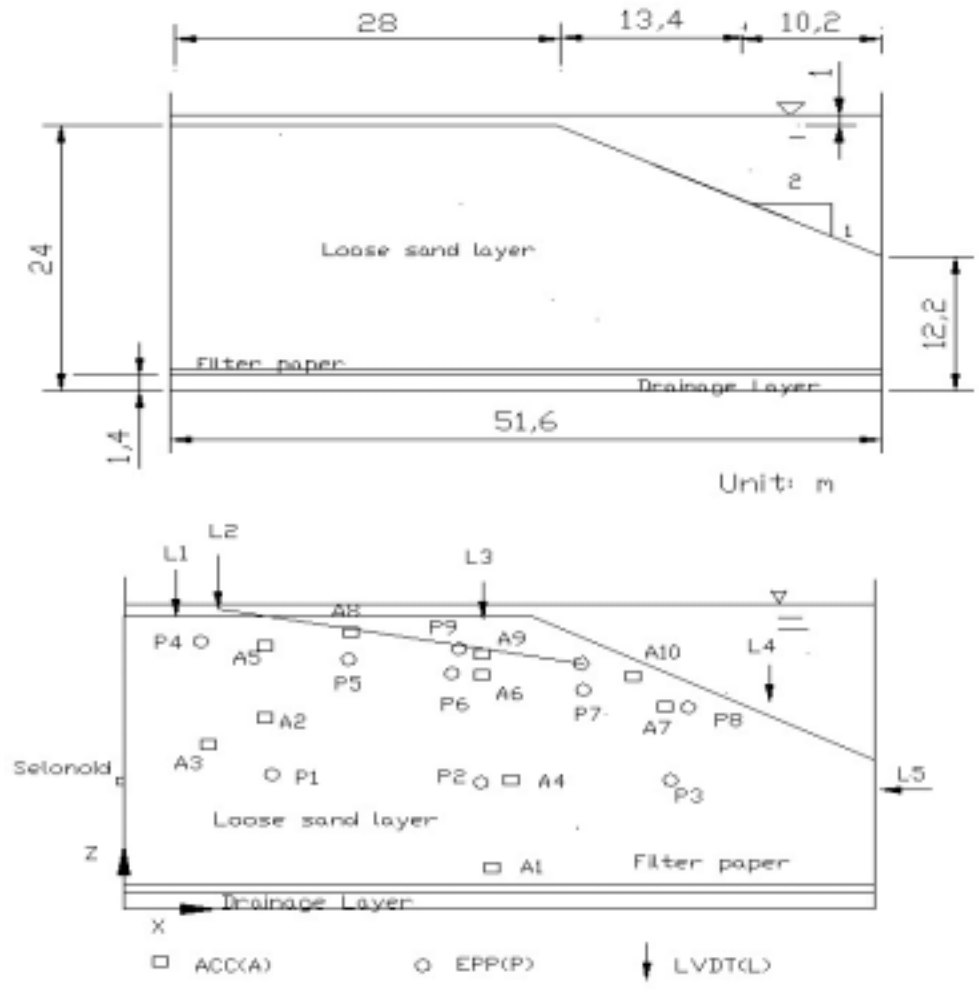


Figure 1. Geometry and instrumentation layout of LRICT6 given by C-CORE

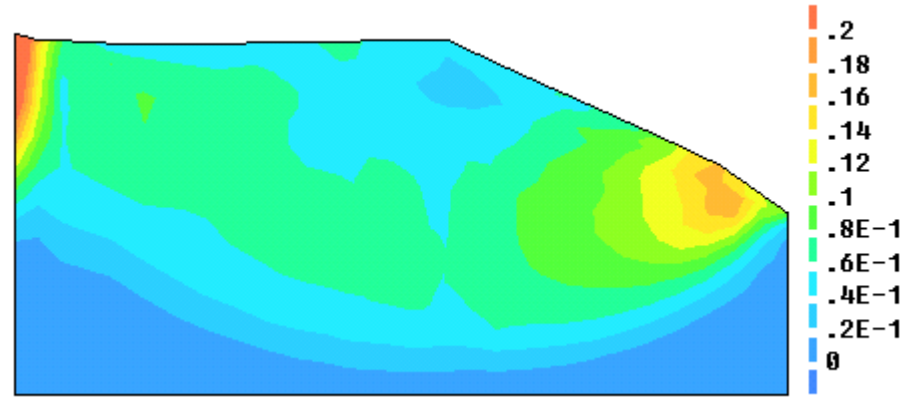


Figure 2. Predicted maximum shear strain contours at t=42.56 s
(Deformed shape magnification factor= 1)

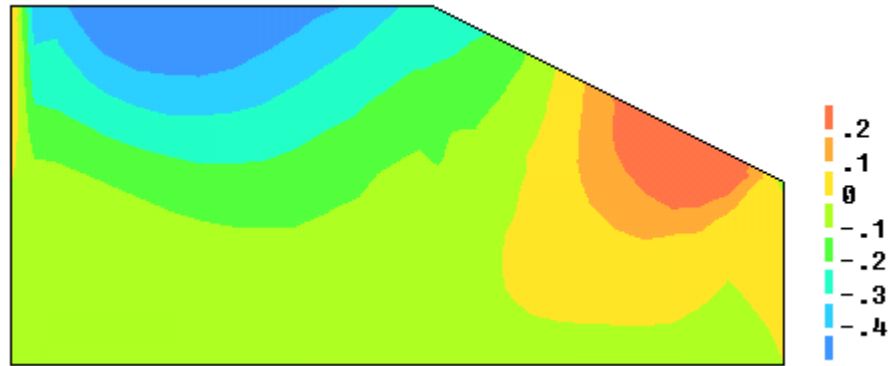


Figure 3. Predicted vertical displacement contours at t=42.56 s

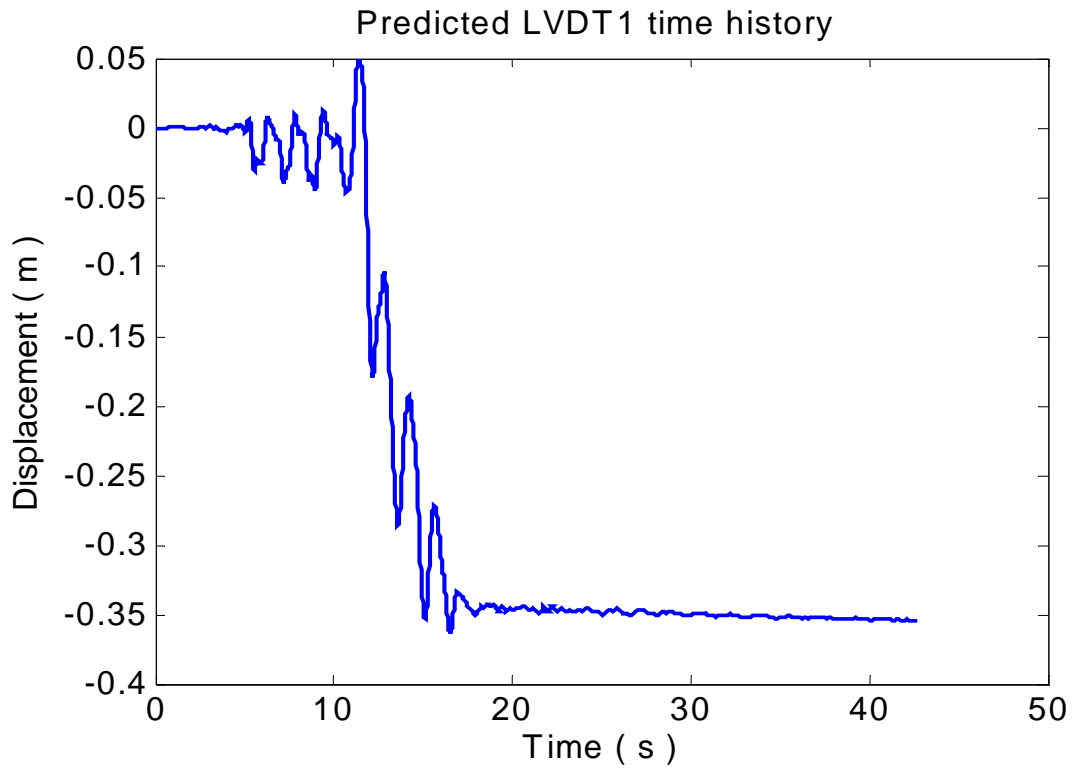


Figure 4. Predicted vertical displacement time history at LVDT1

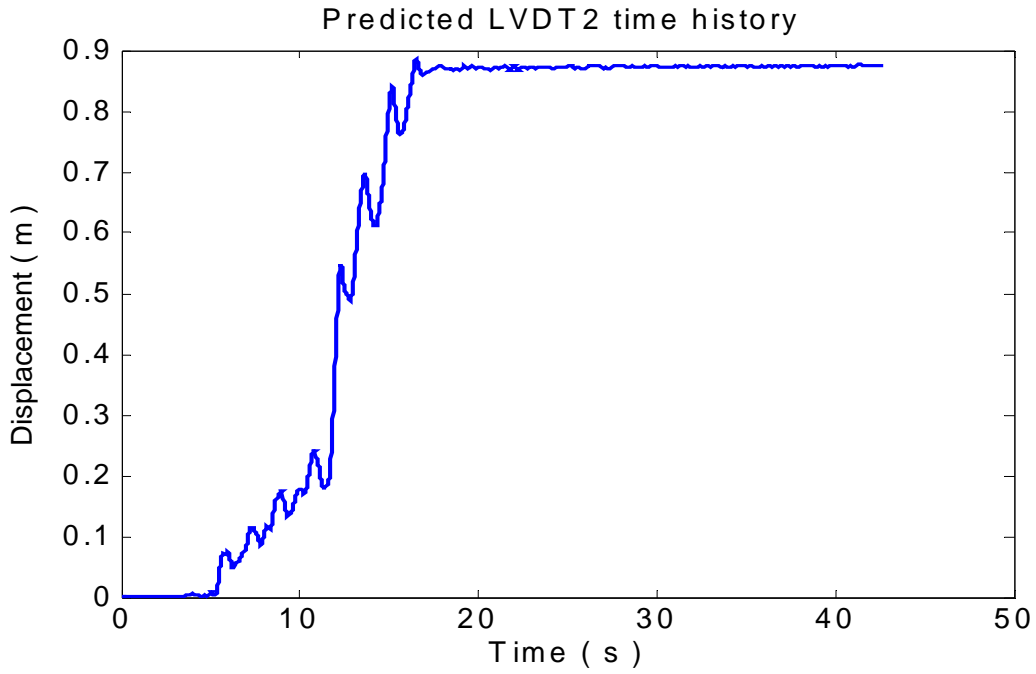


Figure 5. Predicted total displacement time history at LVDT2

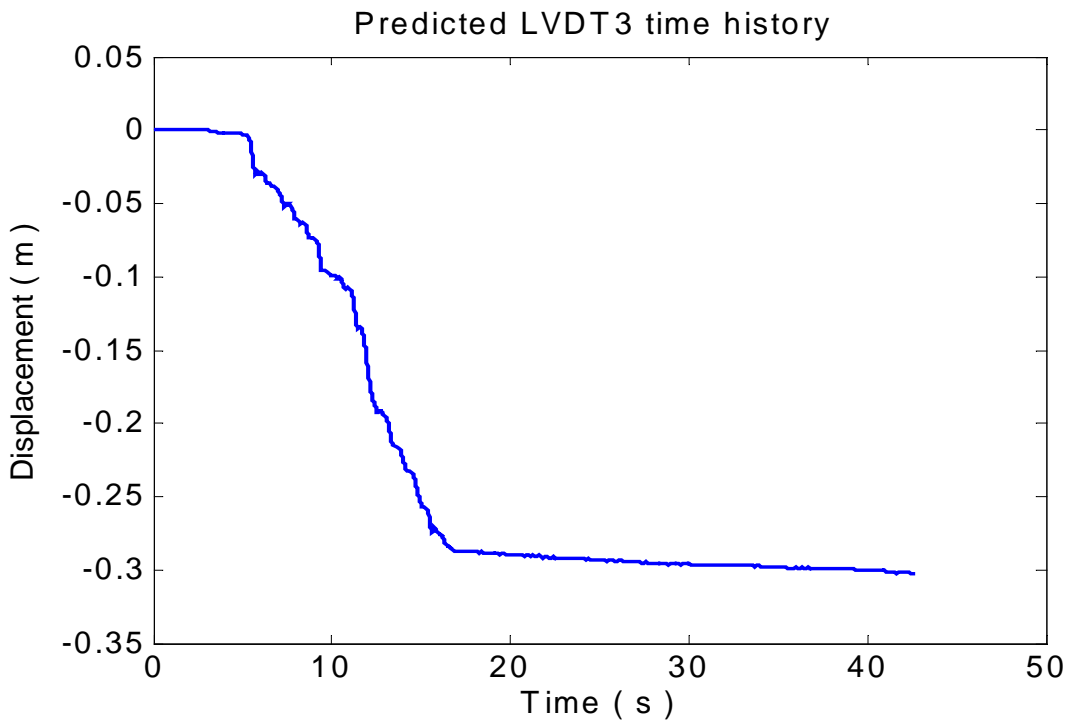


Figure 6 Predicted vertical displacement time history at LVDT3

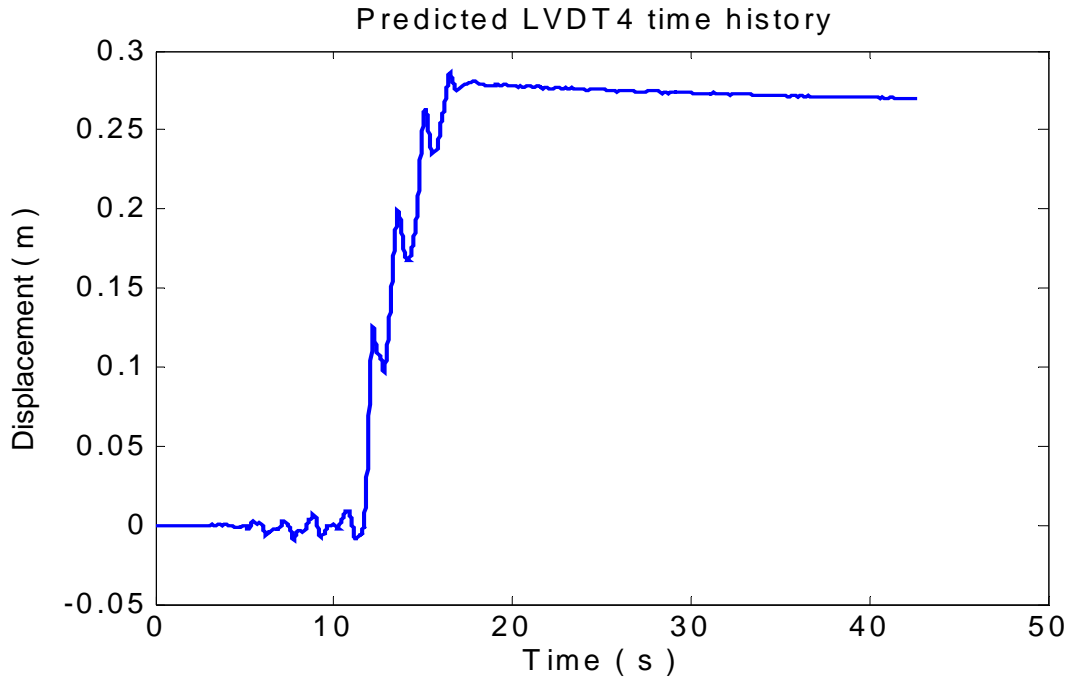


Figure 7. Predicted vertical displacement time history at LVDT4

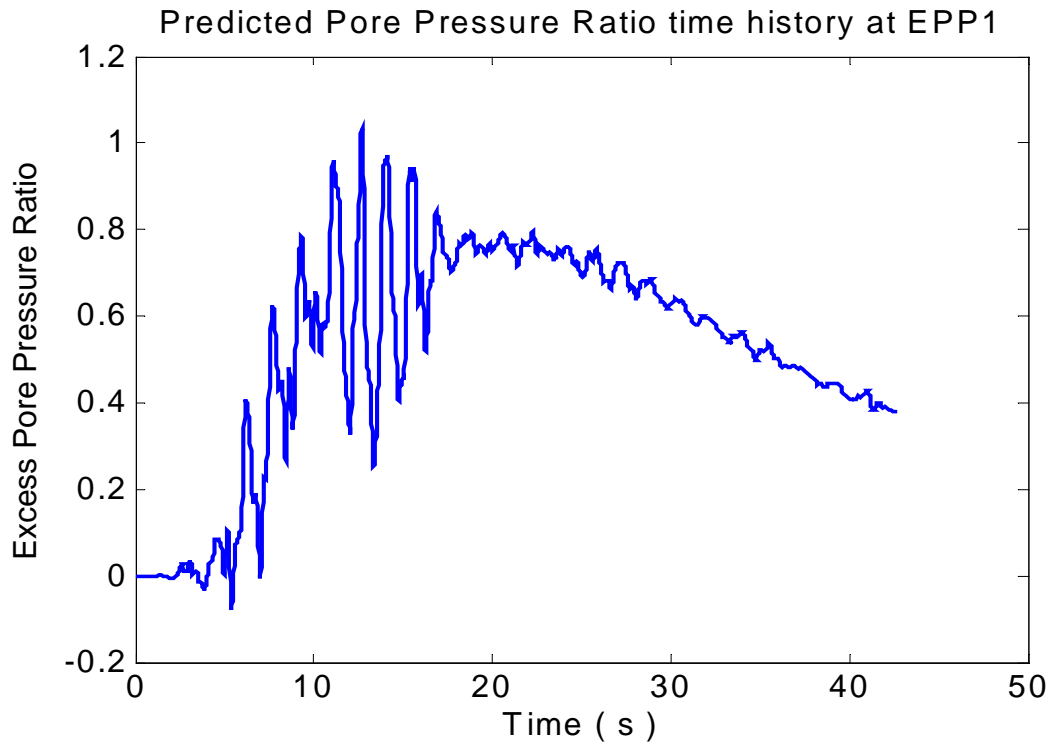


Figure 8. Predicted excess pore water pressure ratio time history at EPP1 (IEVS=123 KPa)

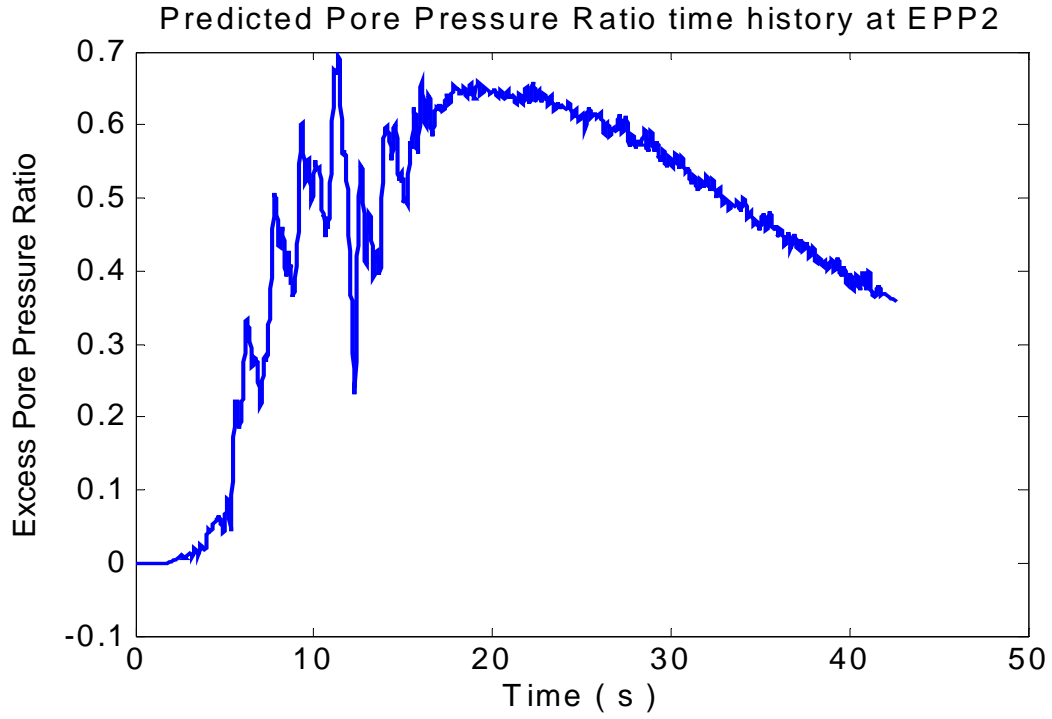


Figure 9. Predicted excess pore water pressure ratio time history at EPP2 (IEVS=120 KPa)

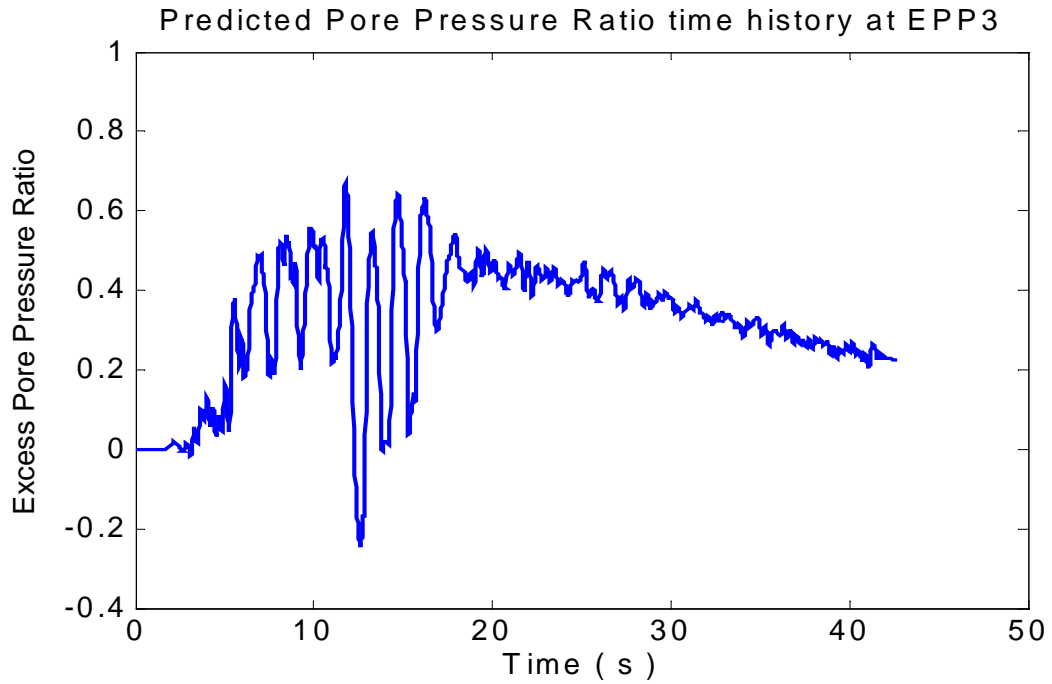


Figure 10. Predicted excess pore water pressure ratio time history at EPP3 (IEVS=88 KPa)

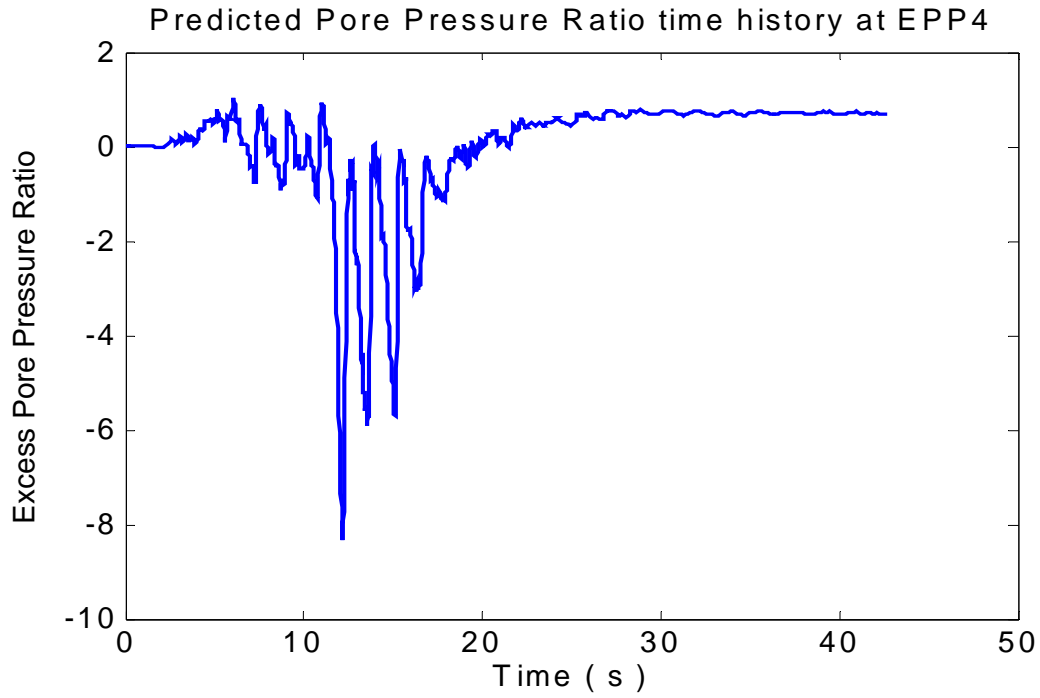


Figure 11. Predicted excess pore water pressure ratio time history at EPP4 (IEVS=12 KPa)

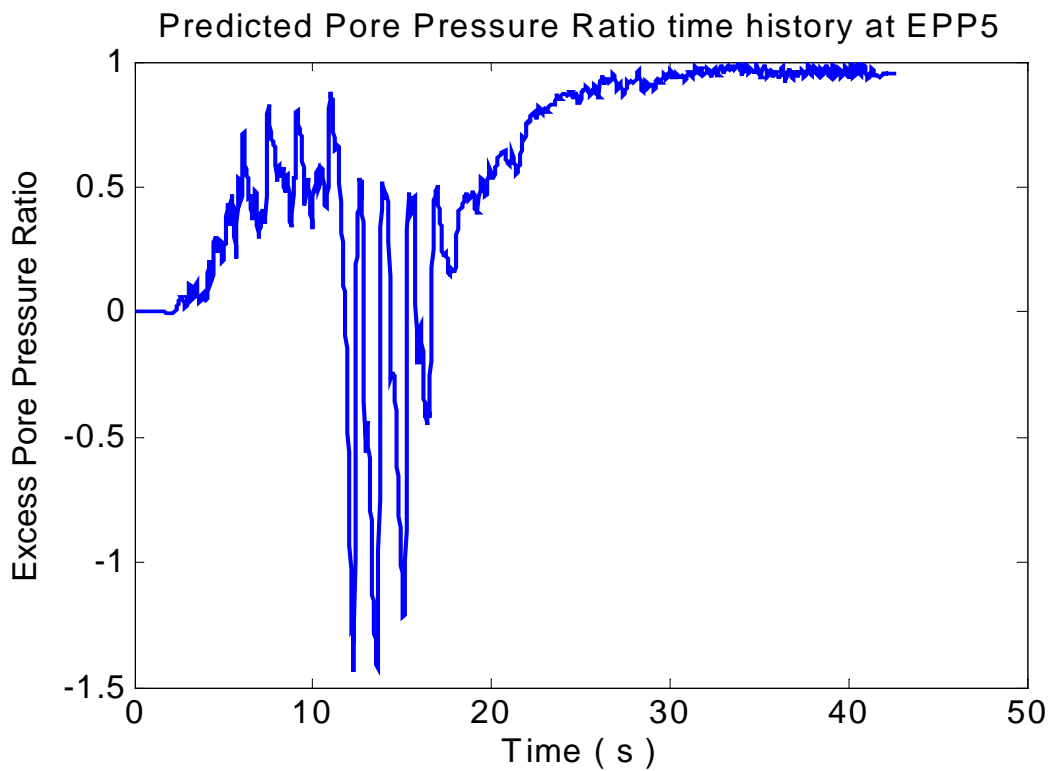


Figure 12. Predicted excess pore water pressure ratio time history at EPP5 (IEVS=25 KPa)

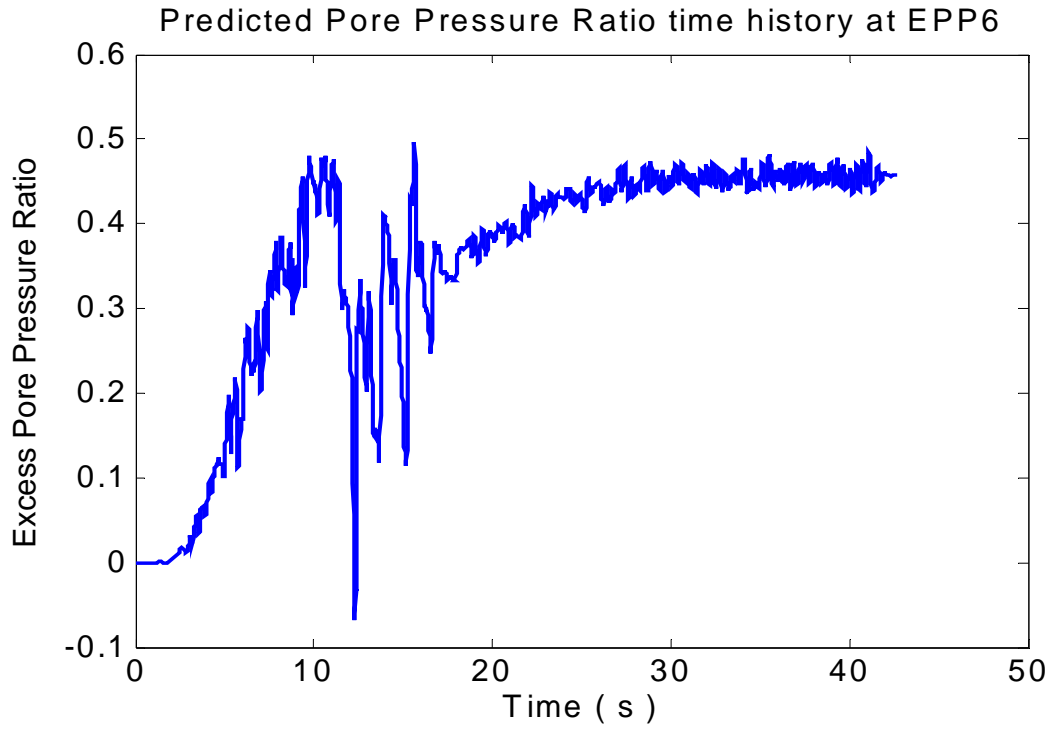


Figure 13. Predicted excess pore water pressure ratio time history at EPP6 (IEVS=58 KPa)

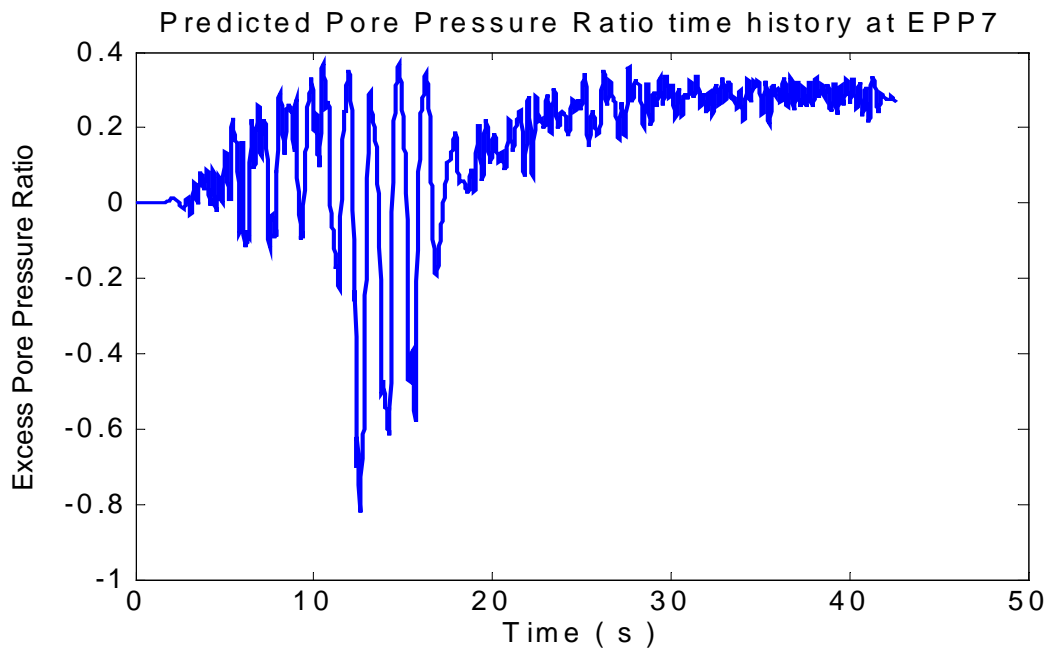


Figure 14. Predicted excess pore water pressure ratio time history at EPP7 (IEVS=35 KPa)

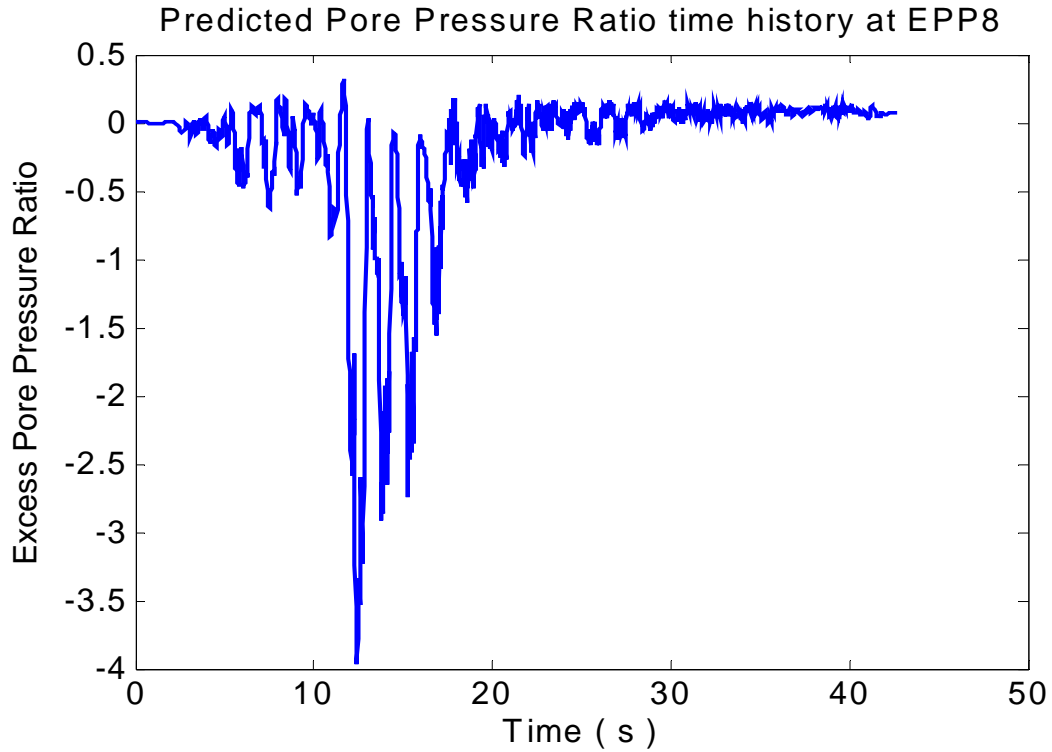


Figure 15. Predicted excess pore water pressure ratio time history at EPP8 (IEVS=16 KPa)

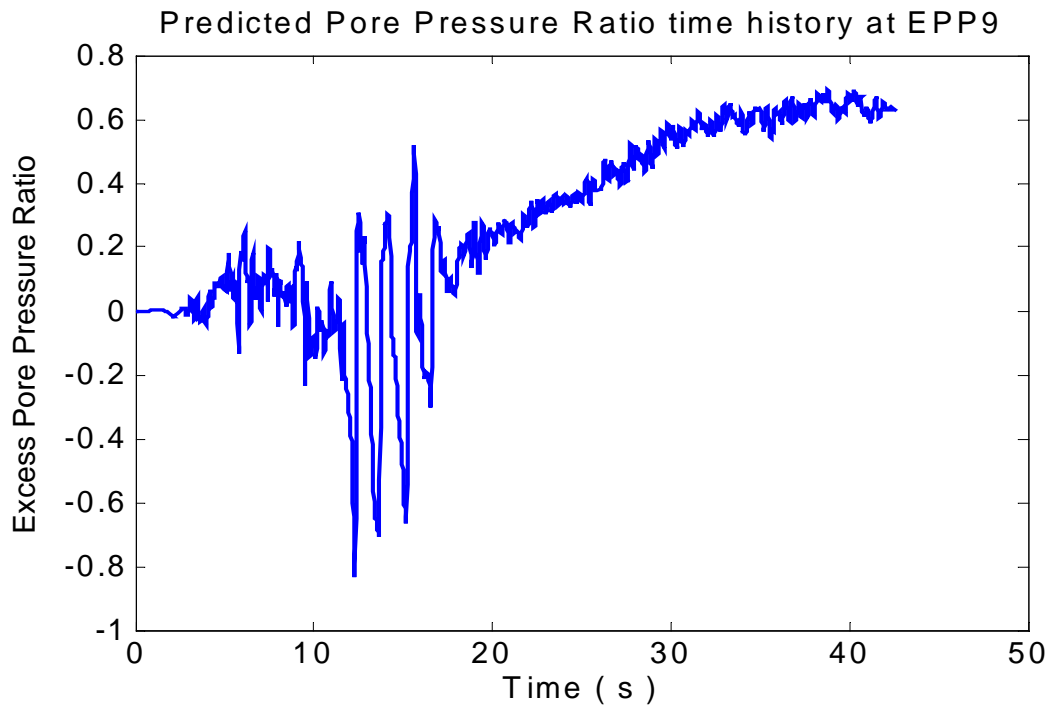


Figure 16. Predicted excess pore water pressure ratio time history at EPP9 (IEVS=13 KPa)

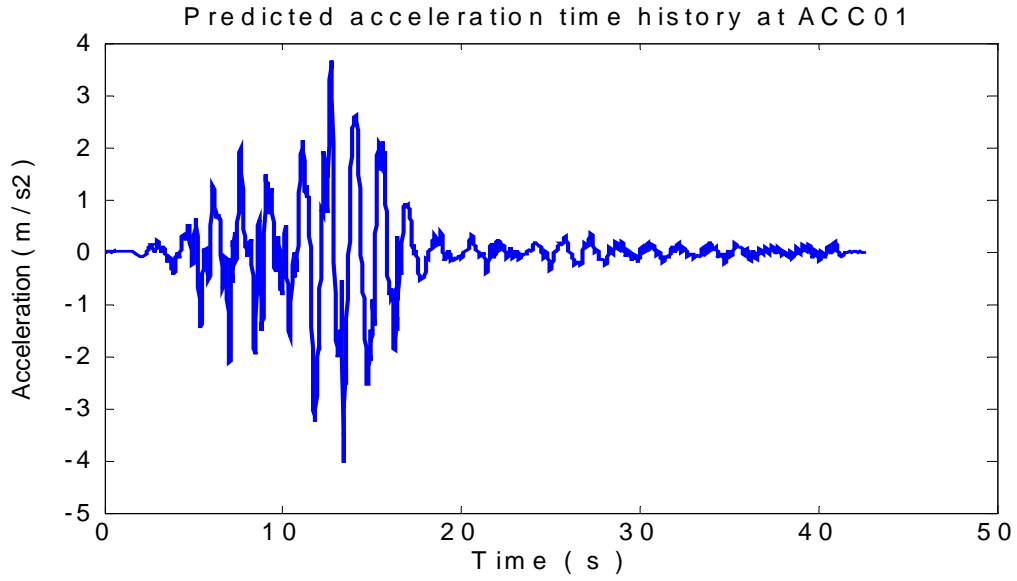


Figure 17. Predicted acceleration time history at ACC01

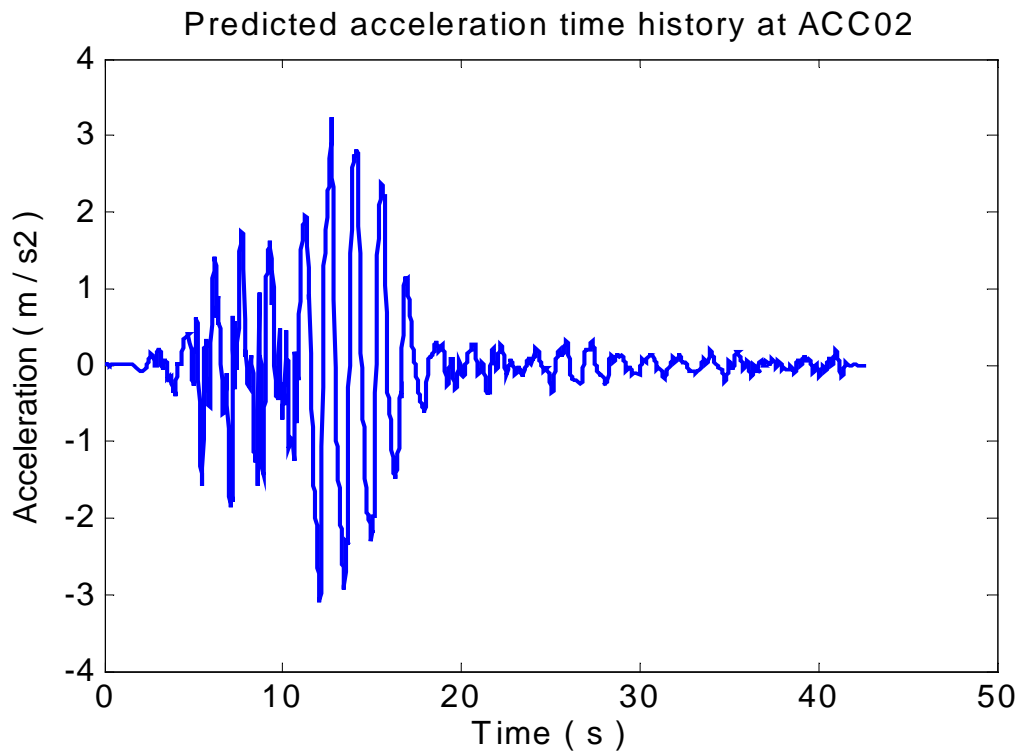


Figure 18. Predicted acceleration time history at ACC02

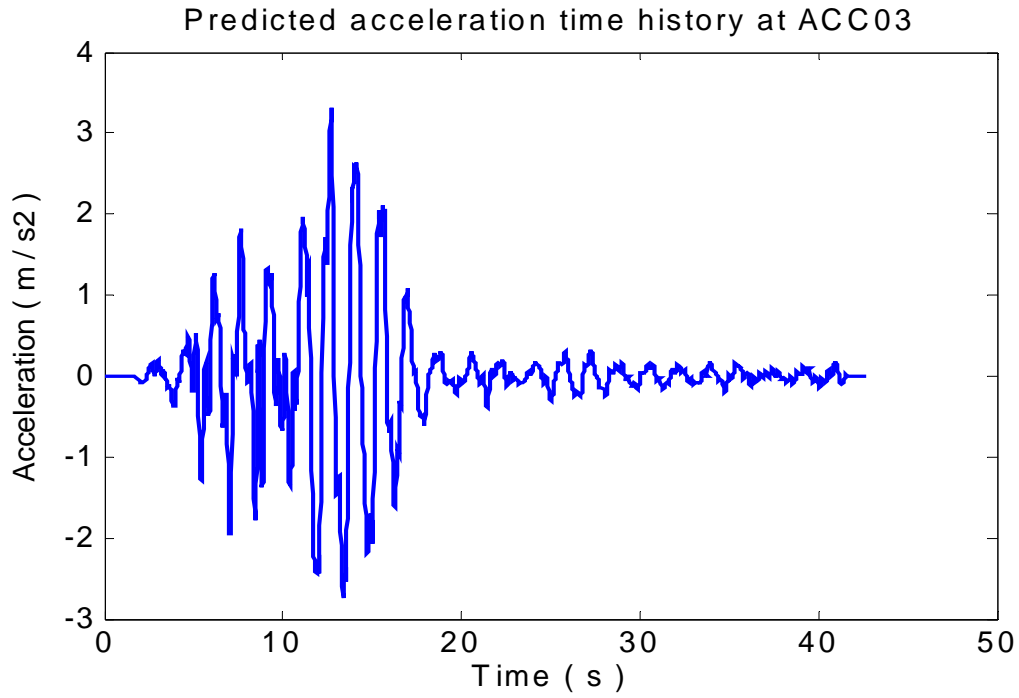


Figure 19. Predicted acceleration time history at ACC03

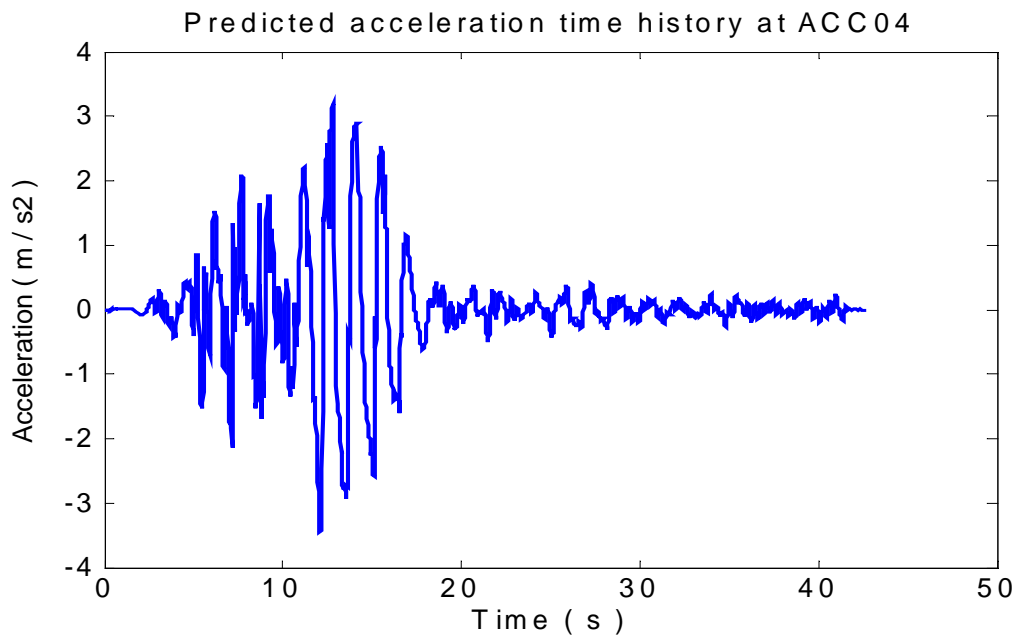


Figure 20. Predicted acceleration time history at ACC04

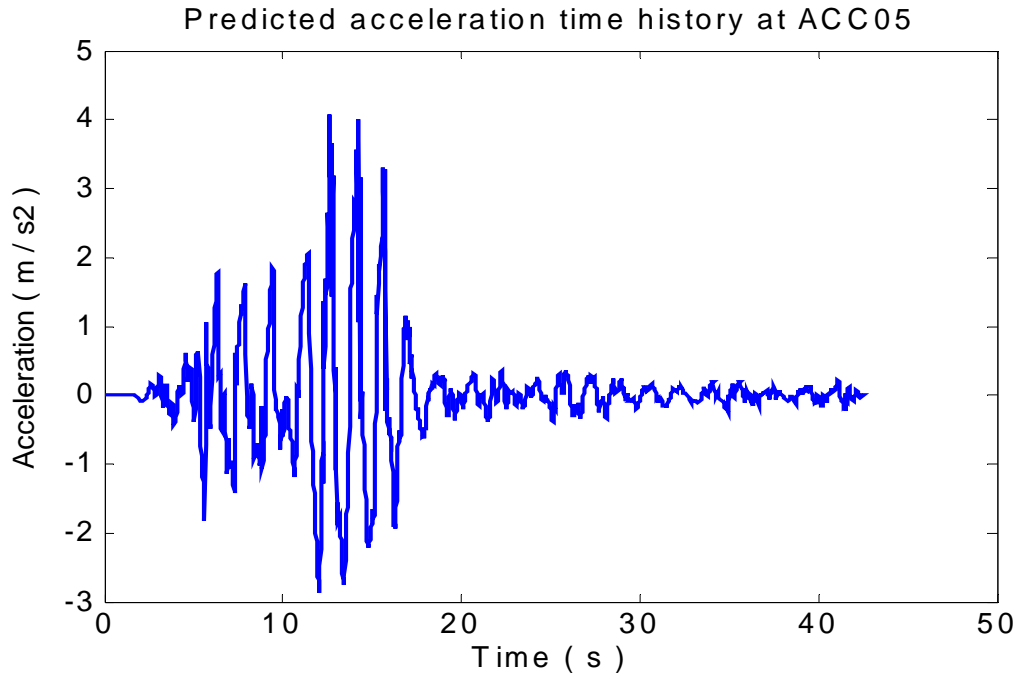


Figure 21. Predicted acceleration time history at ACC05

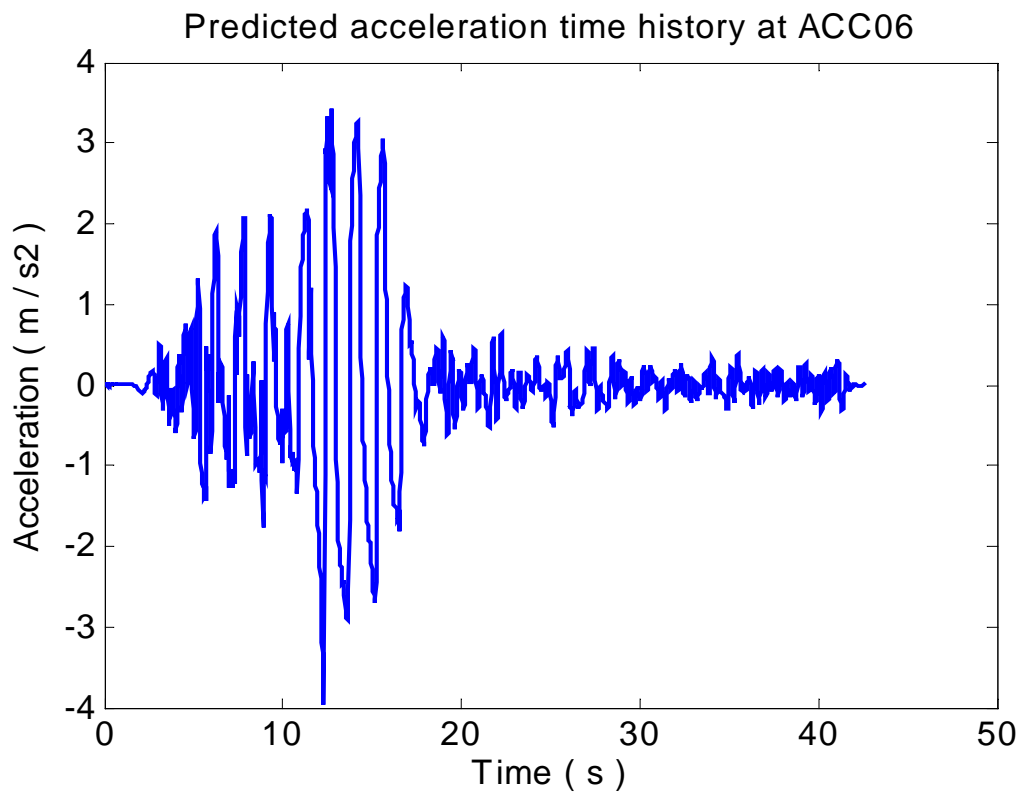


Figure 22. Predicted acceleration time history at ACC06

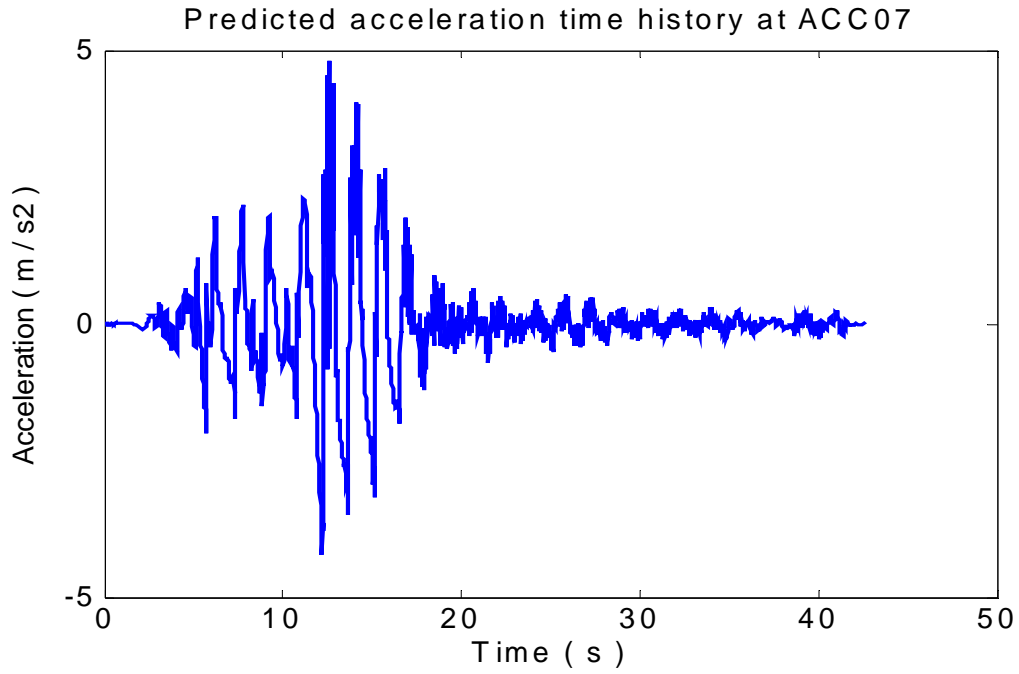


Figure 23. Predicted acceleration time history at ACC07

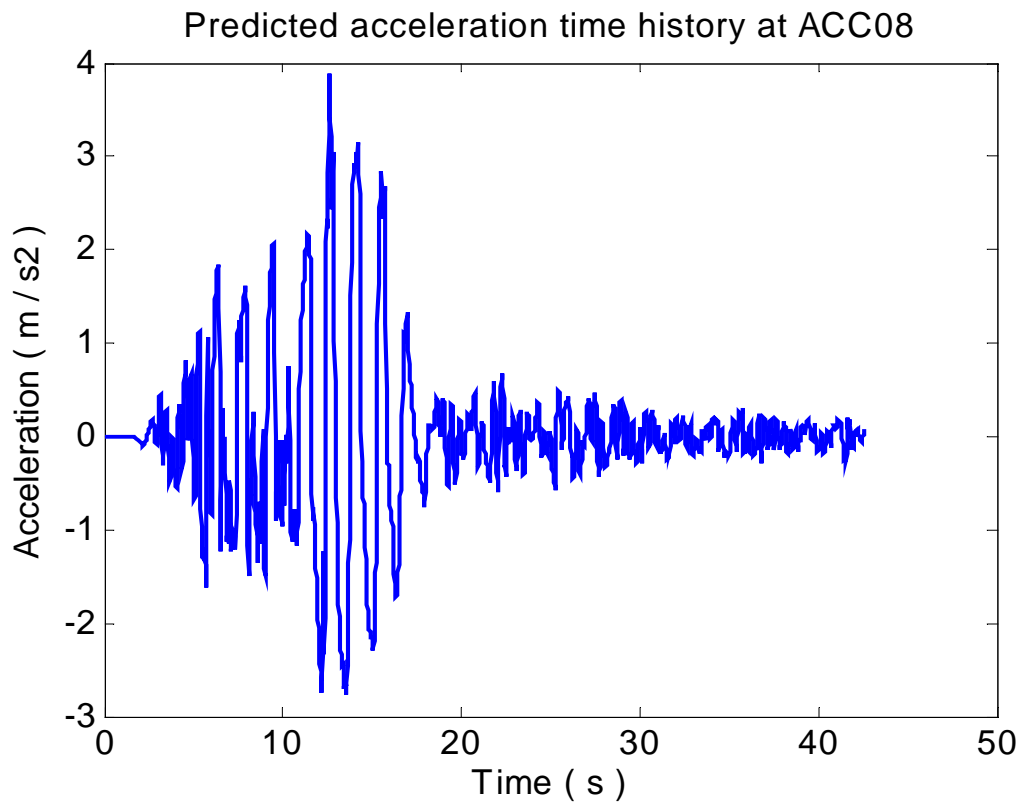


Figure 24. Predicted acceleration time history at ACC08

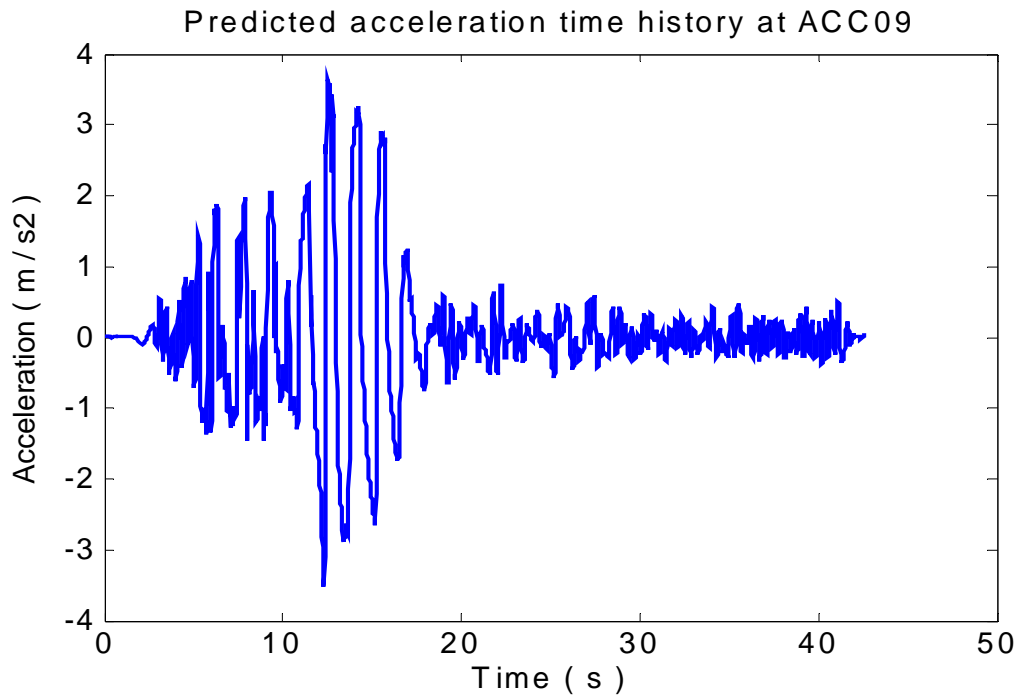


Figure 25. Predicted acceleration time history at ACC09

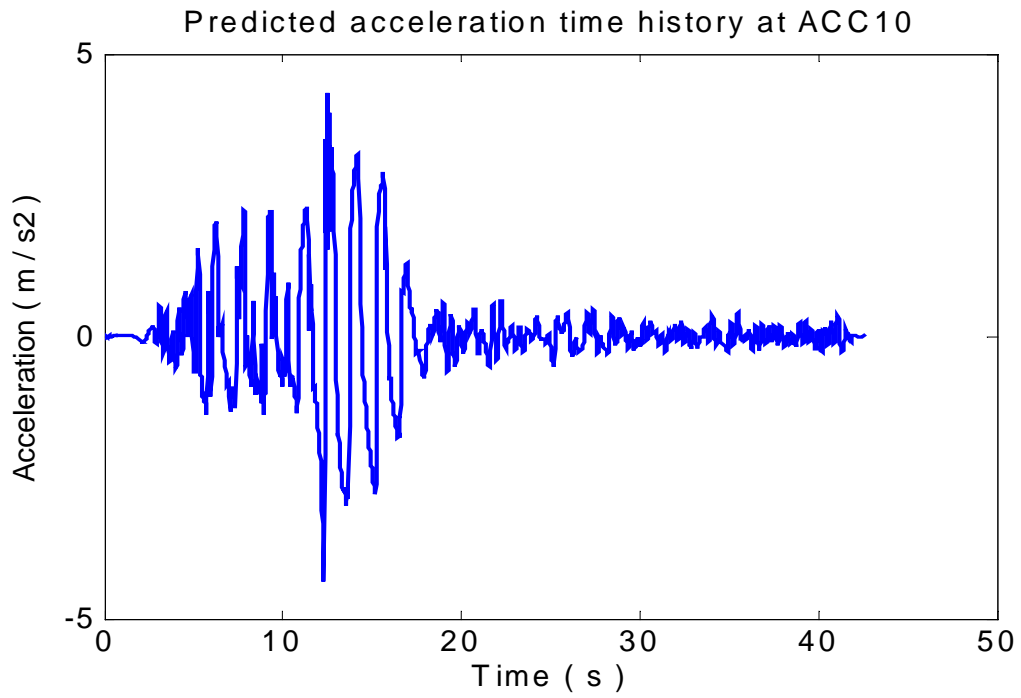


Figure 26. Predicted acceleration time history at ACC10